JOURNAL OF MATERIALS SCIENCE **35** (2000) 2897 – 2905

Nano-structured intermetallic compound TiAl obtained by crystallization of mechanically alloyed amorphous TiAl, and its subsequent grain growth

M. KAMBARA*, K. UENISHI, K. F. KOBAYASHI
Department of Manufacturing Science, Graduate School of Engineering, Osaka University, 2-1, Yamadaoka, Suita, Osaka 565-0871, Japan
E-mail: mk299@eng.cam.ac.uk, uenishi@mapse.eng.osaka-u.ac.jp

The amorphization process during mechanical alloying (MA) was investigated for the Al-50at%Ti and Al-50at%Ti-10vol%TiB_2 powder mixtures. Pure metallic powders of Al and Ti were finely mixed and transformed to the amorphous phase after being milled for about 2880 ks. In the case of Al-50at%Ti-10vol%TiB_2 powder, the amorphous alloys with a fine dispersion of TiB_2 particles could be obtained for a shorter milling times than that required for the powders without TiB_2 ceramics. As a result of heat treatment for the mechanically alloyed amorphous powders, a nanocrystalline intermetallic compound of TiAl (γ) could be produced. Subsequent grain growth of the γ phase during heat treatment was investigated by estimating the grain-growth exponent and the activation energy for grain growth. It was found from this estimation that the grain growth was further suppressed as the powders were mechanically alloyed for longer times. Furthermore, the addition of the TiB_2 particles that could be dispersed during MA finely and homogeneously in the amorphous matrix was found to be effective for suppression of the γ grain growth especially at elevated temperatures as well as for a long annealing. *© 2000 Kluwer Academic Publishers*

1. Introduction

Non-equilibrium alloys and composite materials are expected as new materials to meet the request of recent industrial progress. Especially amorphous alloy in the Ti-Al system has been recognized as one of the most prospective heat-stable materials since it is equipped with the advantages of both high ductility and high weight to strength ratio. However, it has been also considered to include some difficulties in the amorphization process for TiAl alloys by rapid quenching or other conventional techniques in this system. On the other hand, mechanical alloying (MA) was proposed as a new simple technique to yield non-equilibrium materials at lower temperatures [1], which was originally introduced to produce composite powders with a controlled fine microstructure such as oxide dispersion strengthened superalloys (ODS) [2]. Since MA process includes the processes of repeated cold welding and fracturing of mixtures of powder particles, it enables to produce amorphous state as well as fine interdispersion of the ingredients. Furthermore, MA technique is an entirely solid state process, which permits to synthesize non-equilibrium alloys for the reactive alloy elements system such as Al and Ti [3–11]. Therefore, it is expected that a nano-structured composite of the TiAl phase can be produced from the amorphous alloy powders by employing the MA technique.

In this work, aiming at fabrication of nano-structured TiAl alloys, the amorphization process during mechanically alloying was investigated for the Al-50at%-Ti and Al-50at%-Ti-10vol%-TiB_2 systems. Subsequent grain growth process of the TiAl phase (γ) was also investigated quantitatively by evaluating the growth kinetic parameters in order to understand the efficiency of the TiB_2 dispersoid as well as the MA technique.

2. Experimental procedure

Precursor powder mixtures were prepared by using pure Ti (purity: 99.9%, average particle size: 150 μm), Al (99.8%, 20 μm) powders and TiB_2 (98%, 1.7 μm) ceramic powders, maintaining the overall composition of Al-50at%-Ti and Al-50at%-Ti-10vol%-TiB_2. These mixtures were sealed in a cylindrical stainless vial under an argon atmosphere together with hardened stainless balls (12 mm). The ball to powder weight ratio was approximately 100 to 1. The 0.1 cc of methanol was also added into the vial to avoid the adhesion of the powders with balls and vial. MA process was carried out at room temperature at a rotating speed of 90 rpm for 180,

---

[*] *Present address*: Department of Engineering, University of Cambridge, IRC, Madingley Road, Cambridge, CB3, UK.

0022–2461

360, 720, 1440 and 2880 ks. The mechanically alloyed powders were annealed at a heating rate of 0.33 K/s to the temperatures of 973 K, 1173 K and 1273 K and held for various annealing periods. Microstructure of the mechanically alloyed powders and the annealed powders were investigated by scanning electron microscopy (SEM) and transmission electron microscopy (TEM). The powders embedded in epoxy resin were sliced into a thin layer with 30 nm in thickness and used for TEM observation. In order to identify the existing phases as well as to estimate the average grain size, the powders were analyzed by X-ray powder diffraction (XRD) with Co-K_α and Cr-K_α radiations. The following Scherrer formula [12] was used to estimate the γ grain size,

$$D = \frac{0.9\lambda}{\beta \cos\theta} \tag{1}$$

where D is the mean grain size, λ is the wavelength of X-ray, θ is diffraction angle and β is the full width of half maximum of the diffraction peak. In this work, diffractions at (111), (200) and (202) faces of the γ phase were used for estimation. Thermal analysis was performed by differential scanning calorimetry (DSC) at a heating rate of 0.33 K/s in an argon flow atmosphere using alumina powder as a reference material.

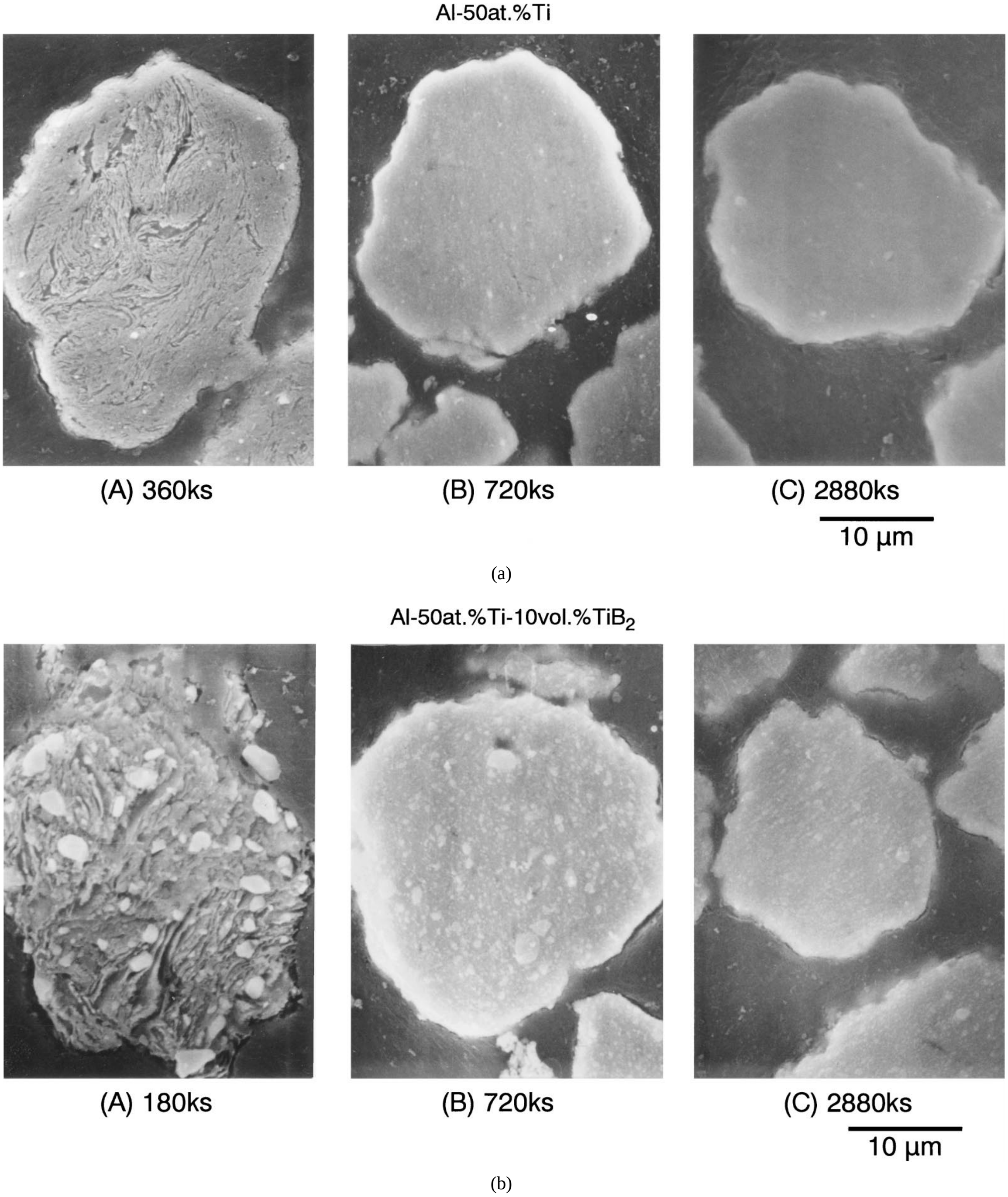

(a)

(b)

Figure 1 SEM images of the powders as mechanically alloyed for various times. (a) Al-50at%Ti and (b) Al-50at%Ti-10vol%TiB_2. In the series of (b), the white contrasted areas correspond to the TiB_2 particles.

3. Results and discussion

3.1. Formation of non-equilibrium and intermetallic phases

Fig. 1a shows the SEM images of the microstructure in the Al-50at%Ti powders as mechanically alloyed. It can be clearly seen that the layered composite structure of starting materials was formed at an early stage of MA, such as 180 ks and 360 ks. As a milling time increases, this layered structure was further refined and convoluted as a result of repetitive kneading effect. After a milling for 2880 ks, no significant structure could be found within the resolution of SEM observation, which is considered to be at the final stage of MA process. Changes of X-ray diffraction patterns with the milling time for the MA powders are shown in Fig. 2a. The diffraction peaks of Al and Ti phase became gradually broader and smaller with increasing the MA time. These peaks were still remained slightly after 1440 ks of milling, but they were completely disappeared and the only broad peak was found after 2880 ks milling. On the other hand, morphological change with MA time in the microstructure of the Al-50at%Ti-10vol%TiB_2 powder seems to be similar to that of the Al-50at%Ti powder mixtures as shown in Fig. 1b. The layered structure was observed at the early stage of MA, which was gradually refined and convoluted with increasing the milling time. It can be also found that the TiB_2 particles represented in white contrasted area became refiner and distributed more homogeneously in the matrix. Change of XRD patterns of these powders also shows the similar tendency with that of the TiB_2 free powders as shown in Fig. 2b. The sharp peaks of TiB_2 phase as well as Al and Ti phases became smaller and broader as the MA time increases, and when the powder was mechanically alloyed for 1440 ks or over, the peaks of Al and Ti disappeared completely and the broader peaks of TiB_2 were only remained. In order to identify the existing phases after 2880 ks milling, the microstructure of both powders with and without TiB_2 particles was investigated by employing TEM spectroscopy as shown in Fig. 3. For both powders with different compositions, any grains of Al and/or Ti phase could not be observed within the resolution of TEM with a beam size of 5 nm. Also, from the electron diffraction patterns, only the halo pattern, which is generally recognized as a typical pattern for amorphous phase, could be found except TiB_2 diffractions in the case of Al-50at%Ti-10vol%TiB_2 powder mixture. Therefore, it can be considered that the amorphous phase was attained after milling at least for 2880 ks for both systems.

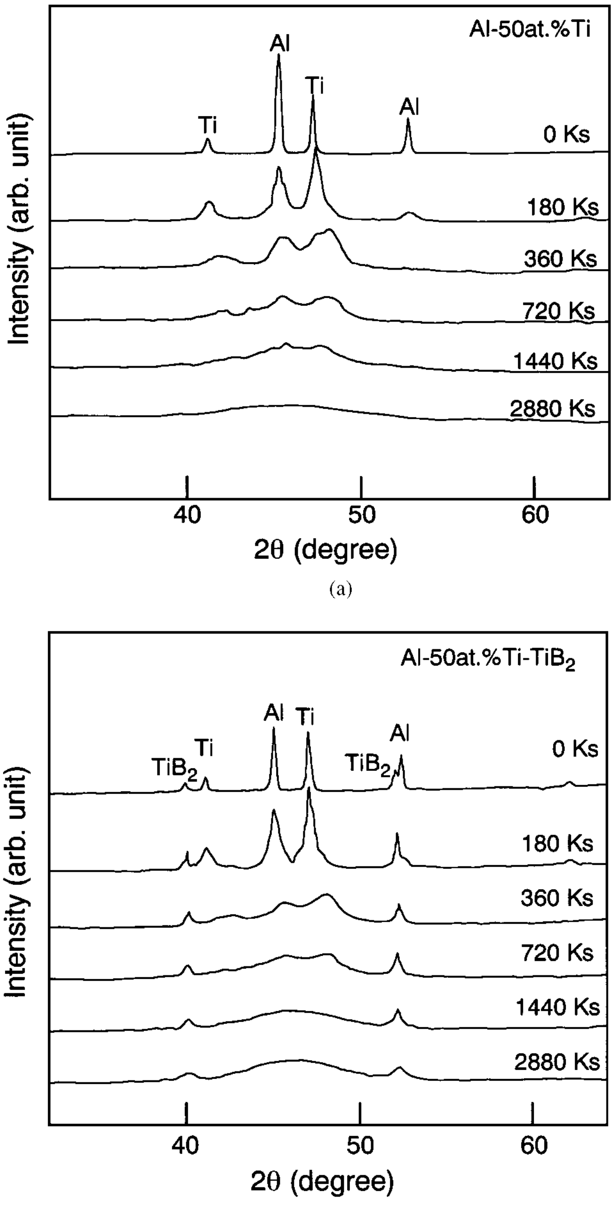

(a)

(b)

Figure 2 Changes of X-ray diffraction patterns of (a) Al-50at%Ti and (b) Al-50at%Ti-10vol%TiB_2 powders as a function of MA time.

Fig. 4 shows the DSC curves of the powders mechanically alloyed for various milling periods. For both the powders with different compositions, two exothermic peaks were found at around 630 K and 730 K for the MA powders of 180 ks milling time, while only one exothermic peak was observed at around 850 K for the MA powders milled for 2880 ks. In order to identify the origin of these exothermic reactions, XRD analysis was carried out for the samples which were continuously heated up below and above these temperatures of each exothermic peak. In the case of the powder added with TiB_2 particles mechanically alloyed for 180 ks, the diffraction patterns annealed at 698 K and 813 K are shown in Fig. 5 comparing with that of the powder as mechanically alloyed. It is apparently found that the γ phase appeared at 698 K and α_2 phase exists at 813 K together with the γ phase. Therefore, it is confirmed that the exothermic peaks at 630 K and 730 K were due to the formations of γ and α_2 phases from the mixture of the pure Ti and Al powders, respectively. On the other hand, XRD patterns for the MA powders continuously heated up to 973 K as displayed in Fig. 6 shows an interesting feature for the powders milled for 2880 ks. That is, although the temperature of the exothermic peak is almost the same between the two different powders, only the α_2 phase was found for the TiB_2 free powder while the γ phase mainly exists with a slight amount of the α_2 phase in the TiB_2 doped sample. These results could in turn indicate that the both powders alloyed for 2880 ks that transformed into γ and/or α_2 phases after annealing are surely an amorphous state

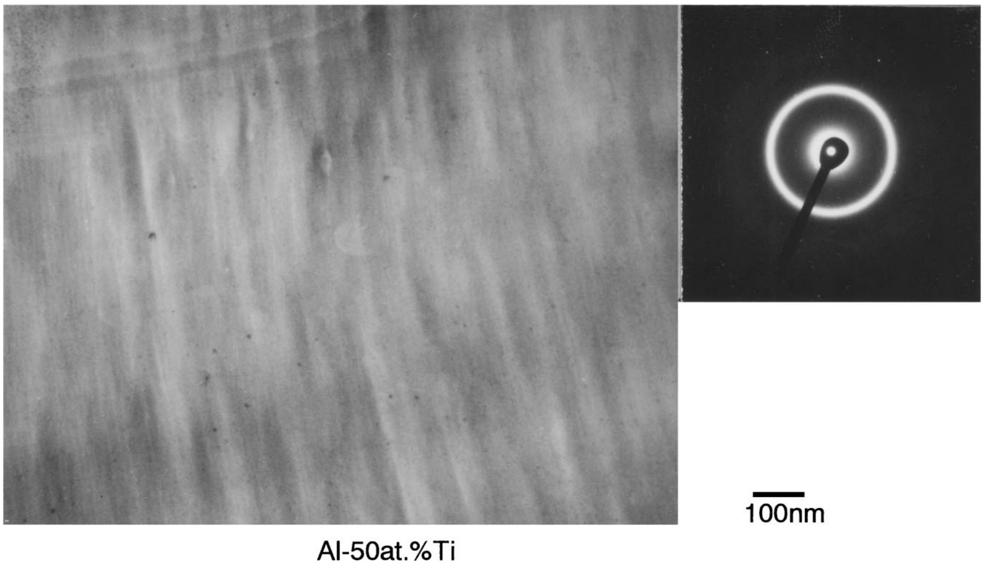

(a)

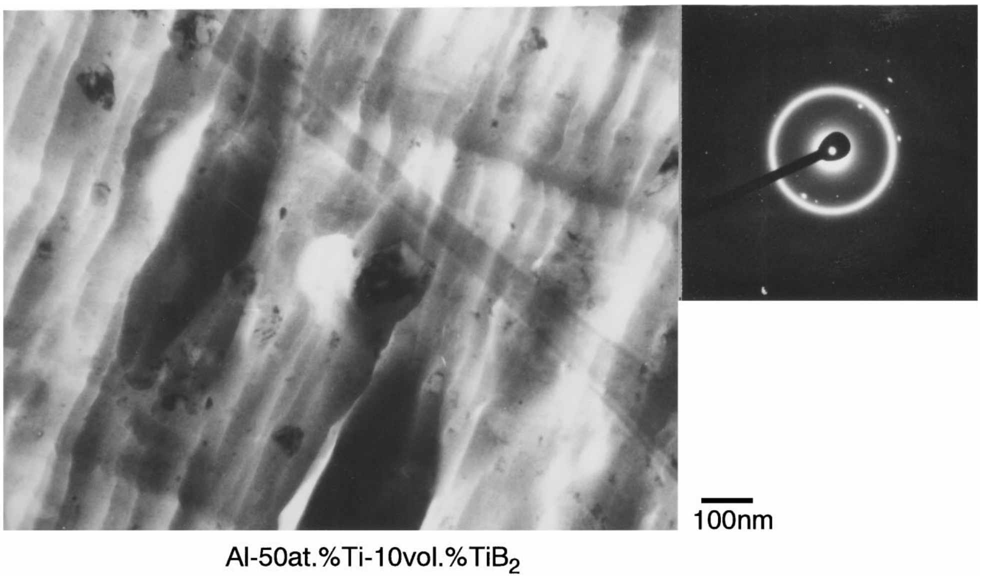

(b)

Figure 3 TEM images and diffractions of (a) Al-50at%Ti and (b) Al-50at%Ti-10vol%TiB$_2$ powders mechanically alloyed for 2880 ks. Black contrasted spots correspond to the TiB$_2$ particles.

and hence exhibit the same temperature of exothermic reaction, i.e., crystallization of amorphous, which is in a good agreement with the literature [11]. For the powders milled for 180 ks, compared with the samples annealed at above and below the temperature of the endothermic peak around 900 K, no significant difference could be found in the XRD patterns. Therefore, it is plausible that the evaporation of hydrogen originally contained in methanol is responsible for these endothermic peaks and it has no strong relation with the transformation of amorphous powders.

In order to understand the results that different phases were crystallized from the amorphous phase at the same temperature of 850 K in the MA powders with and without TiB$_2$ particles, these samples were annealed at different temperatures for several holding periods. Fig. 7 shows the change of diffraction patterns with the holding time for both samples annealed at 971 K. It is clearly found from Fig. 7a that the α_2 phase was gradually transformed into the γ single phase with increasing the annealing time in the case of the Al-50at%Ti sample. A similar tendency can be found in the case of the TiB$_2$ doped sample as shown in Fig. 7b. It is found that the peaks of α_2 phase became smaller with annealing time and finally they disappeared completely and transformed into the γ single phase after being held for 3.6 ks. Furthermore, Fig. 8a and b show the XRD patterns of the samples that were continuously heated up to the higher temperatures of 1173 K and 1273 K, respectively. It can be found in the both powders with different compositions that the peaks of the α_2 phase no longer exist and the γ single phase has already produced just after the continuous heating. These results imply that the α_2 phase appeared as a metastable phase during the crystallization from the amorphous phase to the γ stable phase. In other words, the α_2 phase is at a relatively higher energy hierarchy than the γ phase. Therefore, when the amorphous powders are given a certain thermal energy during annealing and/or a mechanical energy through mechanical alloying process,

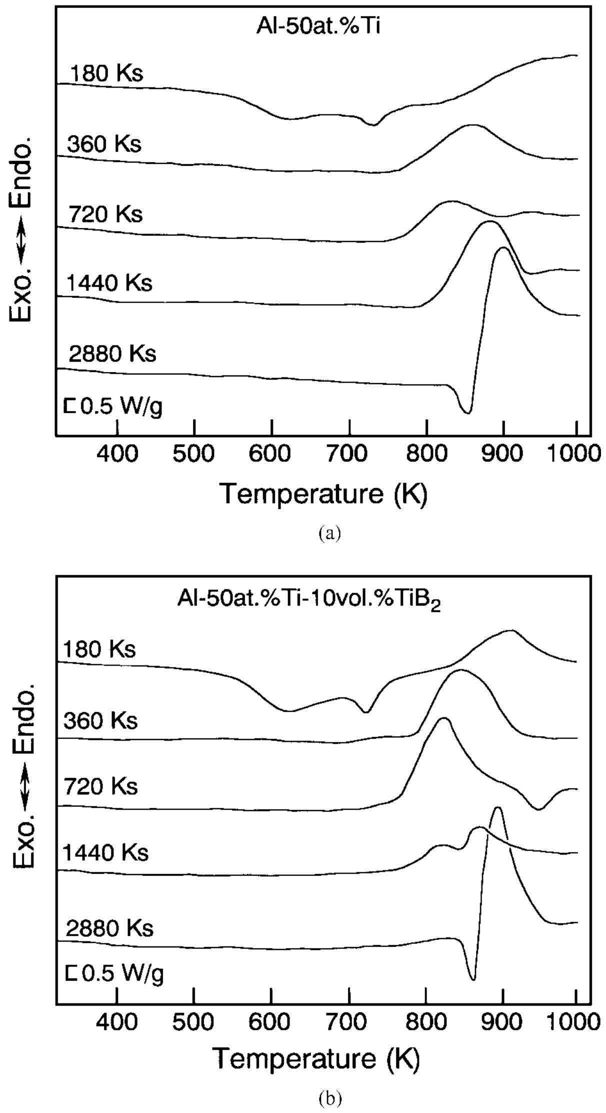

(a)

(b)

Figure 4 DSC curves of (a) Al-50at%Ti and (b) Al-50at%Ti-10vol%TiB_2 powders as a function of MA time.

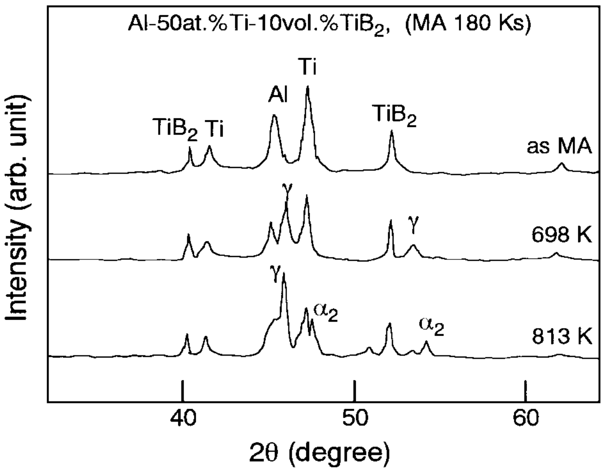

Figure 5 X-ray diffraction patterns of Al-50at%Ti-10vol%TiB_2 powders which were mechanically alloyed for 180 ks and continuously heated up to various temperatures.

the amorphous phase could be crystallized directly into the γ phase without showing any α_2 phase. It can be also considered from Fig. 6 that the addition of the TiB_2 particles can enhance the kneading and convolution effect of MA pronouncedly and introduce more mechanical energy into the amorphous phase.

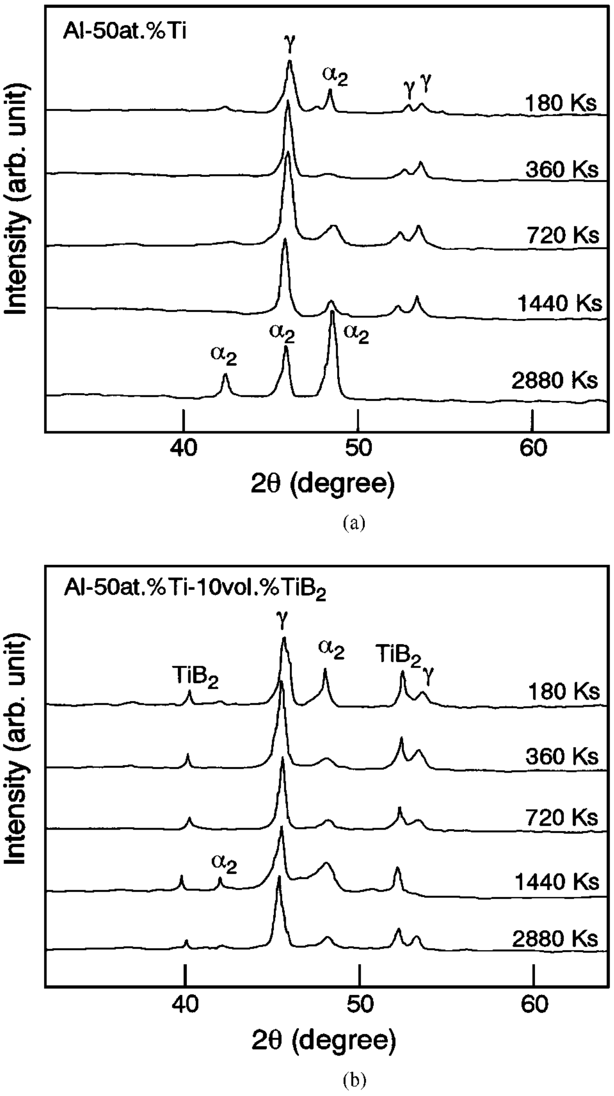

(a)

(b)

Figure 6 X-ray diffraction patterns of the MA powders continuously annealed up to 973 K. (a) Al-50at%Ti and (b) Al-50at%Ti-10vol%TiB_2.

3.2. Grain growth of nanostructured phase

It was found that a single intermetallic γ phase could be produced by means of MA for a long milling time and a subsequent annealing at higher temperatures in the precious section. In order to evaluate the efficiency of the γ grains produced by the MA process and of TiB_2 dispersoid, annealing time dependence of the γ grain size was investigated using the powders mechanically alloyed for 2880 ks. The grain size was measured from the XRD patterns by employing Scherrer formula, and the γ peaks at differentangles were used to minimize the effect of the residual elastic stress on the size calculation. For both powders with and without TiB_2 particles, the γ grain size was estimated to be about 25 nm after a continuous heating up to 975 K. On the other hand, the γ grains represented in black contrasted area in the TEM images as shown in Fig. 9 are also estimated to be about 25 nm, which is roughly in an agreement with that measured from XRD patterns. It is therefore considered that the estimation

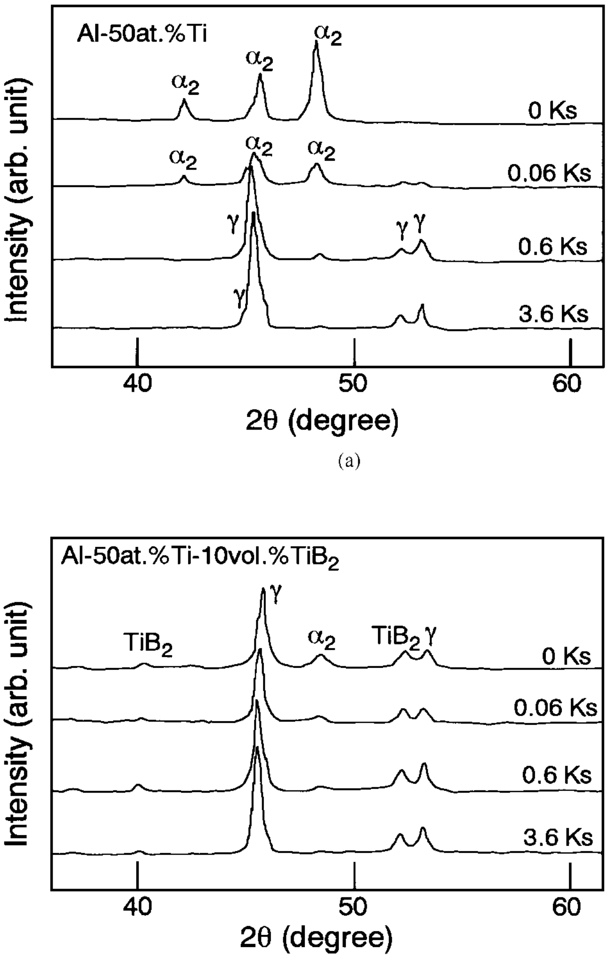

(a)

(b)

Figure 7 Change of X-ray diffraction patterns with annealing time for the (a) Al-50at%Ti and (b) Al-50at%Ti-10vol%TiB_2 powders. The annealing temperature is 973 K.

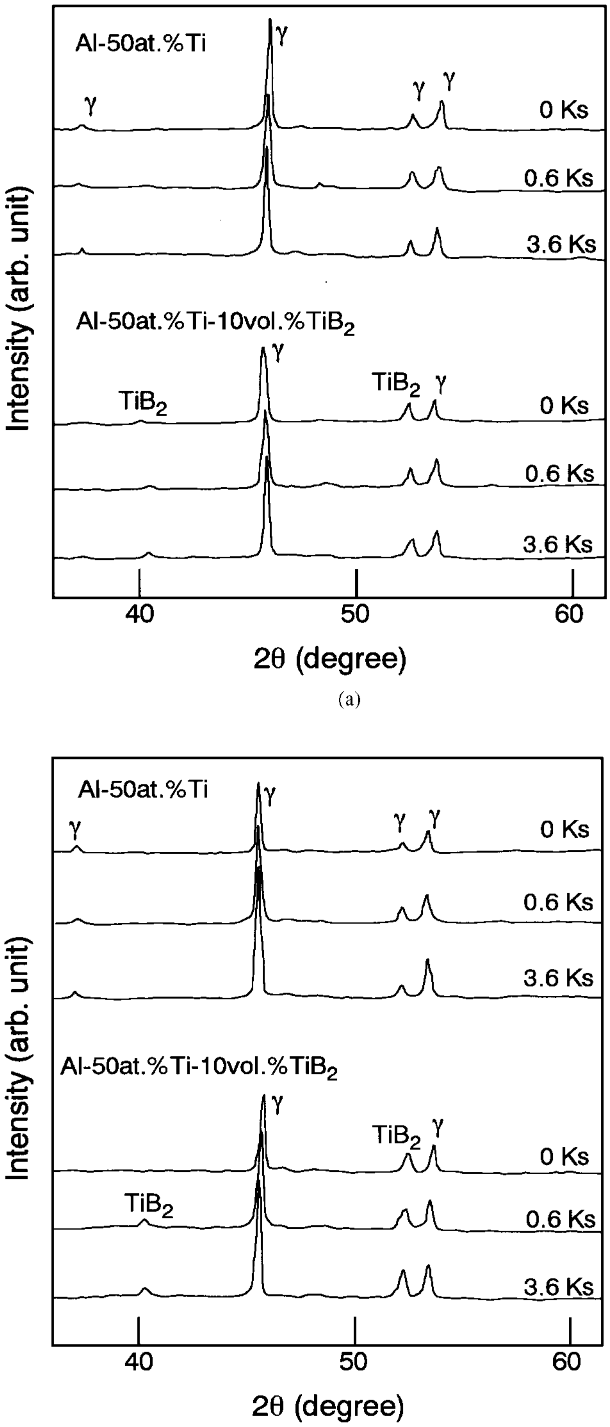

(a)

(b)

Figure 8 Change of the X-ray diffraction patterns with annealing time for the MA powders annealed at (a) 1173 K and (b) 1273 K.

form the XRD patterns could be accurate enough to understand the tendency of the grain growth features. Then, the time dependence of the γ grain size was studied as shown in Fig. 10 in the case of the powders mechanically alloyed for different milling times and annealed for different periods at 973 K. For both Al-50at%Ti and Al-50at%Ti-10vol%TiB_2 systems, it can be found that the γ grain size increased with increasing the annealing time. However, no significant difference in size could be found between the powders milled for different MA times in the case of the Al-50at%Ti powders. On the other hand, once the TiB_2 powders were added, the difference was found pronouncedly, that is, the γ grains that were mechanically alloyed for 2880 ks kept smaller in size compared with that milled for 180 ks and 360 ks especially after a long annealing. The relationship between the grain size and the annealing time at 1173 K and 1273 K was also investigated for the powders milled for 2880 ks, as shown in Fig. 11. It can be found that the γ grains become larger with the annealing time, however, the size of the γ grain in the TiB_2 doped samples is smaller than that of the sample without the TiB_2 particles. It should be further noticed that the coarsening rate of the γ phase in the MA powder with TiB_2, that is represented in a slope of the graph, was found to be lower than that in the MA powder without TiB_2 particles. This means that the TiB_2 dispersoid can play an effective role in suppressing the γ grain growth especially at higher temperatures.

Theoretical and experimental studies on the grain growth process have been intensively carried out so far [13, 14], and Burke and Turnbull have reported a general equation of a parabolic relationship between grain size and time to explain successfully the grain growth features [15]. However, since this relationship is also recognized to satisfy only near the melting point, the following empirical equation has been proposed to

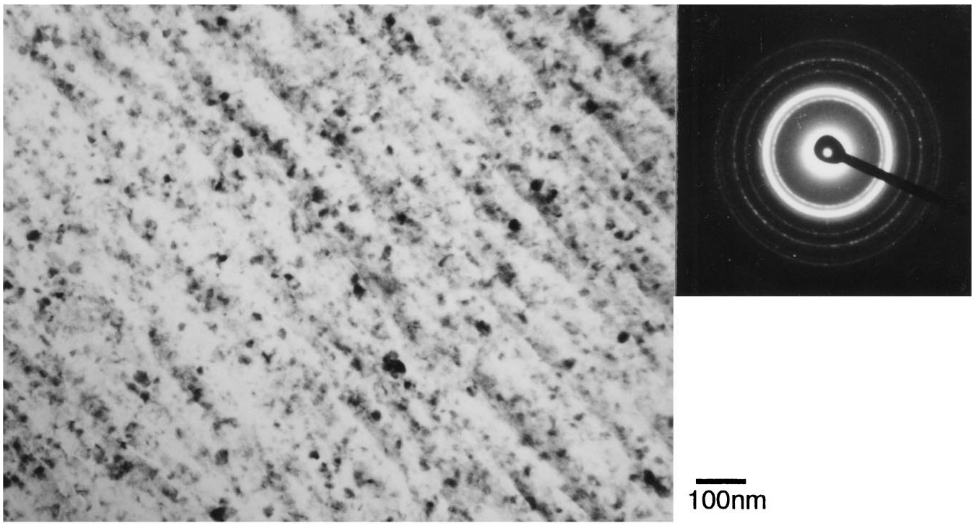

Al-50at.%Ti

(a)

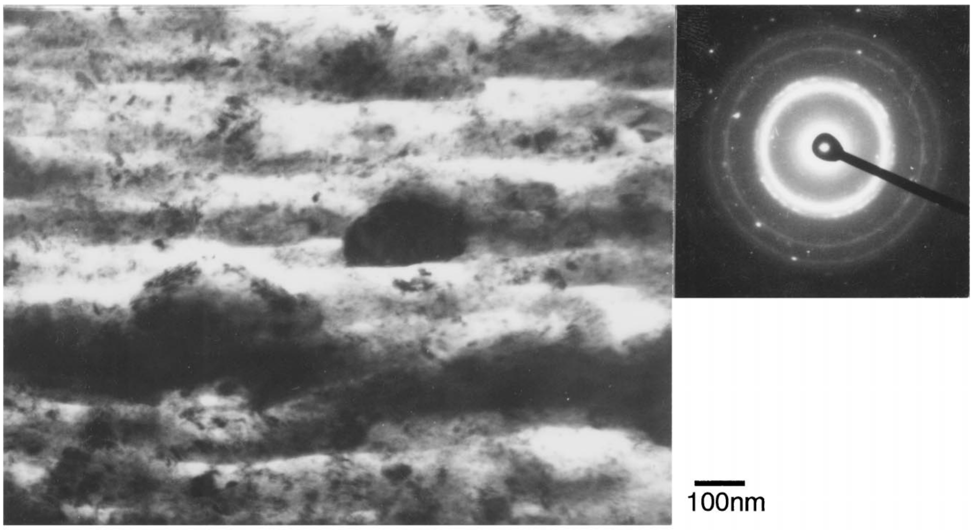

Al-50at.%Ti-10vol.%TiB$_2$

(b)

Figure 9 TEM images and diffractions of (a) Al-50at%Ti and (b) Al-50at%Ti-10vol%TiB$_2$ powders which were mechanically alloyed for 2880 ks and continuously heated up to 973 K.

describe the grain growth mechanism better [16],

$$D^n - D_0^n = Kt \tag{2}$$

where D, D_0 and n are the mean grain size at time t, mean initial grain size, and the grain-growth exponent, respectively. K is a constant that satisfies the following equation,

$$K = -K_0 \exp\left(\frac{-Q}{RT}\right) \tag{3}$$

where Q is the activation energy required for grain growth and K_0, R and T are constant, gas constant and temperature, respectively. A variety of n values has been reported for various systems and discussed to understand the physical meaning by proposing different theories. Although a general principle to explain the variety of n values has not been established especially for grain growth from nanocrystalline alloys, the n value can be a useful factor to describe the difference in growth mechanism between the different systems. In this work, the grain growth exponent and the activation energy were estimated to discuss the grain growth kinetics.

Generally in order to calculate the n values, the following equation can be developed from Equation 2 when the grain size D could be recognized to be enough large to neglect the initial grain size D_0,

$$n \log D = \log K + \log t. \tag{4}$$

Then the values of n and K can be easily obtained by plotting $\log D$ as a function of $\log t$. However, it is obvious from Fig. 11 that since the grain size D of the γ phase after annealing for 3.6 ks is still not enough large to neglect the initial grain size D_0, i.e. at the beginning of annealing, it would be unreasonable to apply the above equation to the present study. Therefore, the following equation was developed from Equation 2 and

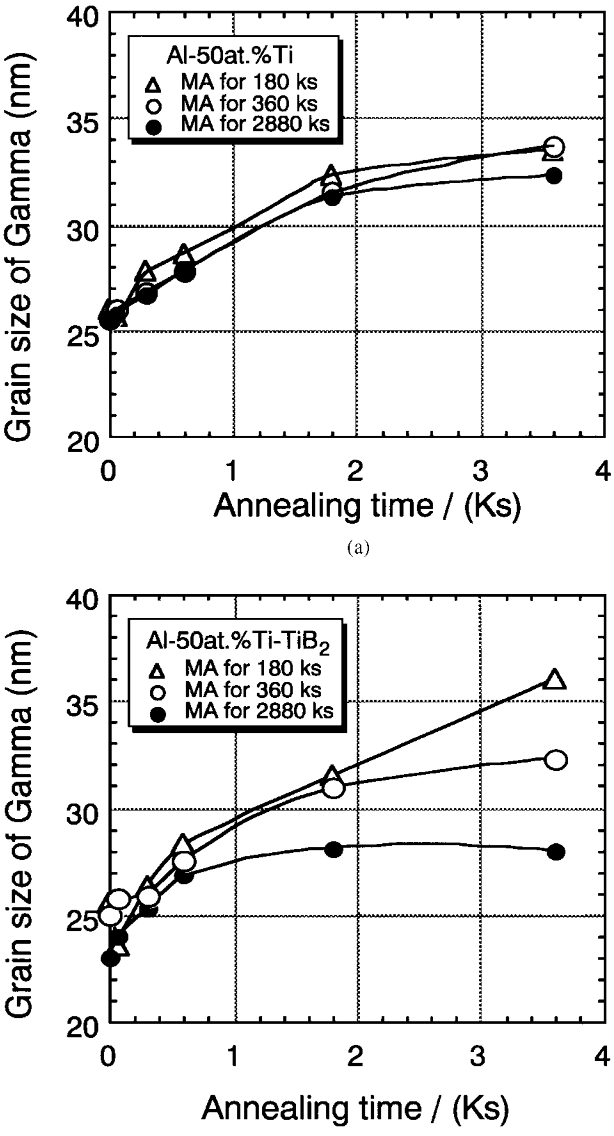

(a)

(b)

Figure 10 Changes of γ grain size with annealing time for (a) Al-50at%Ti and (b) Al-50at%Ti-10vol%TiB$_2$ powders mechanically alloyed for various times, and annealed at 973 K.

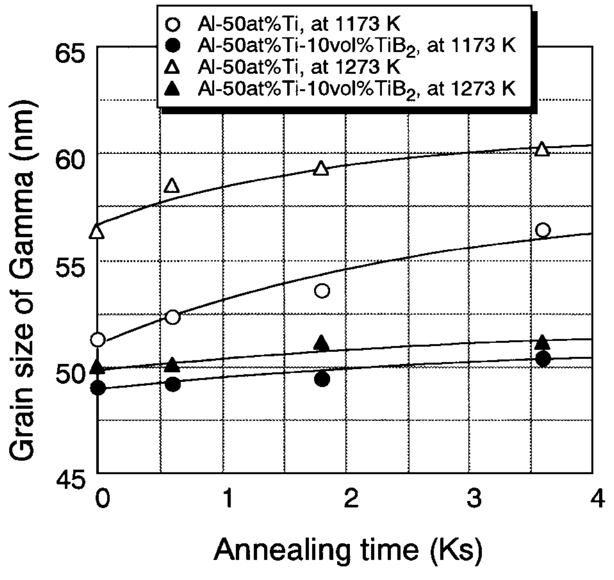

Figure 11 Changes of γ grain size as a function of holding time for the MA powders mechanically alloyed for 2880 ks and annealed at 1173 and 1273 K.

TABLE I Calculated grain-growth exponent; n of the γ grain in the powders mechanically alloyed for 2880 ks

Annealing temperature	Grain-growth exponent: n Al-50at%Ti	 Al-50at%Ti-10vol%TiB$_2$
973 K	8.9	12.1
1173 K	15.6	38.3
1273 K	16.6	44.3

TABLE II Calculated activation energies required for grain growth of the γ grains

	Activation energy
Al-50at%Ti	292.7 kJ/mol
Al-50at%Ti-10vol%TiB$_2$	1994.4 kJ/mol

used to evaluate the n value in this work,

$$\log\frac{\mathrm{d}D(t)}{\mathrm{d}t} = -(n-1)\log D(t) + \log K - \log n. \quad (5)$$

The value of $\mathrm{d}D/\mathrm{d}t$ can be estimated from the Figs 10 and 11, and the relationship between $\log(\mathrm{d}D/\mathrm{d}t)$ and $\log D$ gives the values of n and K. Also, the activation energy Q can be obtained from Equation 3 by plotting $\log K$ as a function of $1/T$. For both Al-50at%Ti and Al-50at%Ti-10vol%TiB$_2$ systems, the estimated n and Q values are listed in Tables I and II, respectively.

It was found that the n value increased with increasing the annealing temperature, and this tendency was pronounced for the samples with TiB$_2$ particles. On the other hand, the activation energy needed for grain growth of the Al-50at%Ti powder was found to be larger than the reported value (235.2 kJ/mol) [17], and much higher activation energies are required for the grain growth of the MA powder with TiB$_2$ particles. Generally, it is reported that the value of n varies from 2 to 4 corresponding to the different metallic systems [15]. Therefore, it is difficult to develop the physically meaningful explanation for this large deviation from the generally reported values. However, it can be simply derived from Equations 2 and 3 that the larger n and Q values can give the smaller D at a constant annealing time. In other words, the grain growth could be suppressed further when a material has relatively larger n and Q values. Accordingly, at least it can be concluded that the grain growth of the γ phase could be suppressed effectively when the samples were produced by the mechanical alloying technique. Also, this effect could be more enhanced by the addition of TiB$_2$ particles since this ceramic dispersoid could be distributed finely and homogeneously at the grain boundaries to prevent the γ grain from growing further.

4. Conclusion

Amorphous alloys were produced by mechanical alloying in the Al-50at%Ti and Al-50at%Ti-10vol%TiB$_2$ systems and a nanocrystalline intermetallic compound of γ phase could be obtained through crystallization of the amorphous alloy so produced by applying a certain thermal energy. As a result of investigation of the relationship between the grain size and the annealing time, the grain growth exponent and the activation energy needed for the grain growth were found to be larger than those of TiAl alloys produced by the conventional method. These results indicate that the grain-growth of the γ phase could be suppressed effectively by employing MA technique, and this effect would be further enhanced by the dispersion of TiB_2 ceramic particles.

Acknowledgement

The authors would like to express appreciations to Dr. Y. Yasuda and H. Kawaguchi for valuable discussions, to Dr. S. Katayama and Dr. T. Tanaka for use of their facilities.

References

1. C. C. KOCH, O. B. CAVIN, C. G. McKAMEY and J. O. SCARBROUGH, *Appl. Phys. Lett.* **43** (1983) 1017.
2. J. S. BENJAMIN, *Metall. Trans.* **1** (1970) 2943.
3. W. GUO, S. MARTELLI, N. BURGIO, M. MAGINI, F. PADELLA, E. PARADISO and I. SOLETTA, *J. Mater. Sci.* **26** (1990) 6190.
4. L. SCHULTZ, *Mat. Sci. Eng.* **97** (1988) 15.
5. G. COCCO, I. SOLETTA, L. BATTEZZATI, M. BARICCO and S. ENZO, *Phil. Mag.* **B61** (1990) 473.
6. Y. H. PARK, H. HASHIMOTO and R. WATANABE, *Mater. Sci. Forum* **88–90** (1992) 59.
7. R. SUNDARESAN, A. G. JACKSON, S. KRISHNAMURTHY and F. H. FOHES, *Mat. Sci. Eng.* **97** (1988) 115.
8. S. KOBAYASHI and H. KIMURA, *Mater. Sci. Forum* **88–90** (1992) 97.
9. P. NASH, H. KIM, H. CHOO, H. ARDY, S. J. HWANG and A. S. NASH, *ibid.* **88–90** (1992) 603.
10. T. ITSUKAICHI, S. SHIGA, K. MASUYAMA, M. UMEMOTO and I. OKANE, *ibid.* **88–90** (1991) 631.
11. T. ITSUKAICHI, K. MASUYAMA, M. UMEMOTO and I. OKANE, *Funtai oyobi Funtaiyakin* **40** (1993) 265.
12. B. D. CULLITY, “Element of X-ray Diffraction” (Addision-Wesley Pub. Company Inc., U.S.A., 1978) p. 102.
13. Z. JANSSON and M. NYGREN, *Thermochim Acta* **114** (1987) 35.
14. H. V. ATKINSON, *Acta Metall.* **36** (1988) 469.
15. J. E. BURKE and D. TURNBULL, *Prog. Metall. Phys.* **3** (1952) 220.
16. T. SPASSOV and U. KÖSTER, *J. Mater. Sci.* **28** (1993) 2789.
17. F. J. VAN LOO and G. D. RIECK, *Acta Metall.* **21** (1973).

Received 14 July 1998
and accepted 19 November 1999